



On the pressure drop of fluids through woven screen meshes

Fouad Azizi

B.&W. Bassatne Department of Chemical Engineering and Advanced Energy, M. Semaan Faculty of Engineering and Architecture, American University of Beirut, Beirut 1107 2020, Lebanon



HIGHLIGHTS

- Pressure drop through woven meshes have been investigated using “real” fluids.
- Two common theories were used to analyze the results along with a large number of literature data.
- A general correlation for each theory was proposed and the results always fell within $\pm 30\%$.
- If properly employed, the two theories were found to render very similar results.

ARTICLE INFO

Article history:

Received 6 April 2019

Received in revised form 3 June 2019

Accepted 25 June 2019

Available online 26 June 2019

Keywords:

Woven mesh

Pressure drop

Friction factor

Screen

Wire gauze

Flow resistance

ABSTRACT

Quantifying pressure drop for fluids passing through woven screen meshes has been the subject of numerous investigations. All of them rely on one of two major theories that explain the pressure losses in terms of a conceptualized nature of the flow. This paper attempts to compare the two approaches using a large number of new experimental measurements conducted using water flowing through circular conduits in which equidistant woven meshes are inserted. The work was also compared against a large number of measurements extracted from the open literature and obtained using single gauzes and/or tightly packed gauzes.

In contrast to earlier works that focused on narrow ranges of Re and/or accurately predicting their respective experimental measurements, this investigation considers, in total, a set of more than a thousand data points. Two universal correlations, each corresponding to a different theory, were derived using data that spans 60 different screen geometries with fraction open areas ranging between 0.21 and 0.84. These correlations were found to predict the pressure drop over a wide range of Reynolds numbers at an acceptable accuracy. Furthermore, it was found that both theoretical approaches render similar outputs.

© 2019 Elsevier Ltd. All rights reserved.

1. Introduction

Woven wire meshes have been employed in a multitude of flow operations where the control of turbulence is required. They are used either to control and either the production or reduction of large-scale velocity or pressure nonuniformities (Pinker and Herbert, 1967; Roach, 1987; Kurian and Fransson, 2009; Groth and Johansson, 1988). A search of the open literature shows that wire screens have also been used in a multitude of other operations. These range from traditional screening, filtering, noise reduction at valves and/or aircraft landing gear, thickeners and coalescers, to greenhouse insect repellants (Armour and Cannon, 1968; Ehrhardt, 1983; Bailey et al., 2003; Okolo et al., 2019). In addition, they have been employed in more sophisticated operations such as Stirling engine regenerators (Costa et al., 2014), thermoacoustic

refrigerators (Wakeland and Keolian, 2003), catalyst support in oxidation chambers – catalytic wire gauzes – (Kołodziej and Łojewska, 2009), high-efficiency heat exchangers, energy-storage units, solar-receiving devices (Wu et al., 2005), and as static mixers in multiphase reactors/contactors (Al Taweel et al., 2013; Azizi and Al Taweel, 2015). Their usage is further justified by their physical durability as well as their excellent chemical, and thermal resistance.

In all fluid related operations, studies concerned with flow through screens are focused on three main areas, namely, the characteristics of downstream turbulence, the effect of the screen on time-mean velocity distributions, and the pressure drop across the screen (Roach, 1987; Laws and Livesey, 1978). When employing screens in the process industry, the latter parameter remains however of utmost importance to the design engineer because it is directly related to the cost of the operation.

The pressure drop across a woven mesh has been the subject of tens of studies (including but not limited to all aforementioned

E-mail address: fouad.azizi@aub.edu.lb

Nomenclature

a	specific surface area [m^{-1}]	$RMSE$	root mean squared error [-]
B	screen wire diameter [m]	SSE	sum of squared errors [-]
c	constant in correlation [-]	U_o	fluid superficial velocity [$\text{m}\cdot\text{s}^{-1}$]
D_h	hydraulic diameter [m]	U_e	effective or interstitial velocity [$\text{m}\cdot\text{s}^{-1}$]
D_s	equivalent spherical diameter [m]	W	length of a wire segment [m]
f	fanning friction factor [-]	Greek symbols	
$F(Re)$	correlating function [-]	α	fraction open area of screen [-]
f_L	laminar component of friction factor [-]	γ	constant in correlation
f_T	turbulent component of friction factor [-]	Δp	pressure drop [Pa]
$G(\alpha)$	correlating function [-]	ε	screen void volume [-]
K_s	pressure loss coefficient [-]	θ	angle between flow direction and bed axis [deg]
L	bed length of screen sheet thickness [m]	μ	dynamic viscosity [$\text{Pa}\cdot\text{s}$]
L^*	hydraulic dimensionless channel length [-]	ρ	density [$\text{kg}\cdot\text{m}^{-3}$]
L_e	effective bed sheet thickness [m]	τ	tortuosity factor [-]
M	screen mesh size [m]	Subscripts	
Mn	mesh number [m^{-1}]	$K.L.$	related to Kołodziej and Łojewska (2009)
Re	Reynolds number [-]	Wu	related to Wu et al. (2005)
Re_b	Reynolds number based on wire diameter [-]		
Re_h	Reynolds number based on hydraulic diameter [-]		
Re_s	Reynolds number based on equivalent spherical diameter [-]		

references), which attempted to quantify and correlate or predict it. This parameter, however, is highly dependent on the geometry of the woven screen which is characterized by its type of weave, the count of warp and weft wires and their diameters, in addition to the free open area of the screen (Fischer and Gerstmann, 2013). Moreover, there exist different kinds of weaves that are defined by the arrangement of the warp and weft wires with some having an open area in the direction of flow (plain), or in very tightly woven weaves (dutch). The most commonly used types of screens are the plain weave, twill weave (semi-twill, or full twill), fourdrinier weave, and dutch weaves (plain dutch, reverse plain dutch, or twilled dutch). This study is, however, only interested in the simplest type, the plain square mesh, the geometry of which is depicted in Fig. 1. These are geometrically similar gauzes, characterized by warp and weft wires of equal diameters and placed on a square matrix. These screens are then characterized by their wire diameter, b , mesh size, M , and fraction open area, α . The screen mesh size is defined as the center-to-center distance of two adjacent parallel wires.

While attempting to characterize the pressure drop of flow through screens, and except few studies, the majority of investigators conducted experiments using air or idealized situations (e.g., pure fluids) to try and limit the effect of contaminations on their findings, e.g., moisture-free air, or water with no dissolved gases. Discrepancies between the findings still exist and no “universal” correlation to predict the pressure drop could be found in the literature despite the numerous search efforts.

In chemical reactors/contactors, where screens have been successfully employed to promote multiphase contacting between phases to enhance mass transfer and/or reaction operations (Al Taweel et al., 2013; Azizi and Al Taweel, 2015; Al Taweel et al., 2007; Al Taweel et al., 2005), fluids can be far from ideal where only filtered fluids are available. For this reason, it becomes essential to have a large set of measurements conducted under “real” conditions in order to better quantify the operating cost of utilizing screens as static mixers.

The objectives of the current work are therefore to present a new set of experimental measurements conducted using plain-weave

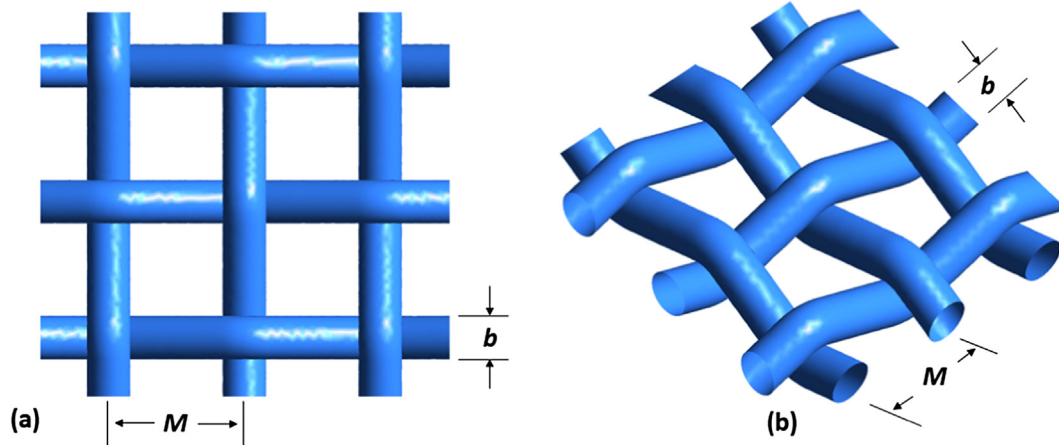


Fig. 1. Geometry of a plain square woven mesh showing both (a) top and (b) axonometric views.

wire mesh screens of various geometries and compare them with existing data from the literature. Also, an attempt to correlate the data and deduce “universal” correlations will be undertaken, and the findings will be compared against various known correlations. In this quest, the two-known theories for quantifying Δp will be presented, utilized, and compared against each other.

2. Methodology

Numerous works on the subject of pressure drop across a wire gauze can be found in the literature with most of them sharing similar objectives, namely, to experimentally investigate the pressure losses for a fluid flow across a screen and attempt to correlate it in order to better explain the reported data (Armour and Cannon, 1968; Ehrhardt, 1983; Pinker and Herbert, 1967; Roach, 1987; Kurian and Fransson, 2009; Wakeland and Keolian, 2003; Kołodziej and Łojewska, 2009; Wu et al., 2005; Brundrett, 1993; de Vahl Davis, 1964; Munson, 1988; Wieghardt, 1953; Ingmanson et al., 1961; Kołodziej et al., 2009; Grootenhuys, 1954; Annand, 1953).

A thorough review of the various approaches used to estimate the pressure drop across a screen was recently presented by Kołodziej et al. (2009). In that study, the authors reviewed the most prominent works in the field and highlighted their theoretical differences. The reader can be referred to their work, or other investigations for more background information (Pinker and Herbert, 1967; Wakeland and Keolian, 2003). It is worth noting that two major theoretical approaches to describing pressure drop across a screen can be found, namely, a fluid dynamics approach and a chemical engineering one. The former is referred to as the “flow-around” approach because it treats the flow through a mesh by analogy to the flow around a cylinder and is commonly used when single screens are employed. Moreover, the latter is referred to as the “flow-through” approach, in which the system is treated as a bundle of tubes and pressure drop correlations follow that of flow through porous media (Kołodziej et al., 2009). This approach is more pronounced in cases where closely stacked gauzes are employed.

Unlike most published works on the subject, the current investigation deals with screen meshes from a chemical reactor design point of view. In these applications, woven meshes are used as static mixers to repetitively superimpose an adjustable, radially-uniform, highly-turbulent field on the near plug flow conditions encountered in high-velocity pipe flows (Al Taweel et al., 2013; Azizi and Al Taweel, 2015; Al Taweel et al., 2007; Al Taweel et al., 2005; Azizi and Al Taweel, 2011). The very high energy dissipation rates generated in the thin region adjacent to the screen mixers as well as the quasi-isotropic turbulence further downstream proved to be very effective in processing multiphase systems and helped in intensifying the rates of mass transfer between phases (Al Taweel et al., 2013; Azizi and Al Taweel, 2015; Al Taweel et al., 2007; Al Taweel et al., 2005; Azizi and Al Taweel, 2011; Azizi and Al Taweel, 2007; Azizi and Al Taweel, 2011; Al Taweel and Chen, 1996). Screens were also used to study the effect of grid-generated turbulence on the development of chemical reactions as well as testing the applicability of micro-mixing models (Bennani et al., 1985; Bourne and Lips, 1991).

In such processes, the use of real fluids is indisputable and therefore knowledge of pressure drop relevant to these conditions is of great importance. In real applications, it would be deemed too costly to have, for example, the ideal condition of a gas-free liquid, or a moisture-free gas, before entering the reactor.

In a previous study, Azizi and Al Taweel (2011) developed a simulation approach for predicting the spatial variation of the

energy dissipation rate downstream of a screen in a one-dimensional domain. In that investigation, the authors also attempted to compare few correlations for the screen drag coefficient against pressure drop data obtained in real systems (Chen, 1996; El-Ali, 2001), as a method of validation of their model. They found that the correlation proposed by Chen (1996), fitted best the experimental results that were obtained using tap water flowing through a channel equipped with a number of equidistant screens, and over a limited set of operating conditions.

This work, however, attempts to employ the two commonly used approaches for flow through screens (i.e., flow through, and flow around) in order to correlate new experimental data and compare the accuracy of the theories and highlight their pitfalls. This study will only present measurements obtained using real systems by compiling a large set of published and previously-unpublished measurements. The findings will then be compared to a plethora of experimental measurements and/or correlations from the open literature that were obtained using either dehumidified gases or degasified liquids.

2.1. Methods for correlating the data

As previously mentioned, two theoretical approaches for calculating the pressure drop across a woven wire mesh exist in the literature, namely, the “flow-around,” and the “flow-through.” The former approach assumes similarity with the flow of fluids around a cylinder, while the latter strikes the analogy with the flow through porous media.

According to the “flow-around” theory and in the majority of studies published in the open literature, pressure drop across a wire mesh has been reported in terms of a screen pressure loss coefficient, K_s . By analogy with other pressure loss coefficients in fluid dynamics, this coefficient is defined as the ratio of the total pressure drop across a screen to the dynamic pressure of the approaching flow, as highlighted in Eq. (1).

$$K_s = \frac{\Delta p}{(1/2)\rho U_0^2} \quad (1)$$

Most studies that investigated this coefficient concluded that it is a function of both Reynolds number and screen open area, with the dependency having the form shown in Eq. (2).

$$K_s = G(\alpha) \cdot F(Re) \quad (2)$$

where G is a function of the fraction open area of the screen, α , sometimes referred to as screen porosity function, and F a function of the Reynolds number. In this context, the screen open area, α , is calculated based on the orthogonal projection of the screen. What remains inconclusive, however, is the form of the function $G(\alpha)$ and the definition of the Reynolds number. Pinker and Herbert (Pinker and Herbert, 1967) were the first to compile and delineate these differences, and their work remained the basis to which most future investigations refer. According to them, and based on an extensive literature survey, the most commonly used forms of $G(\alpha)$ are four and highlighted in Eq. (3).

$$\begin{cases} G_1(\alpha) = \frac{1-\alpha}{\alpha^2} \\ G_2(\alpha) = \frac{1-\alpha^2}{\alpha^2} \\ G_3(\alpha) = \frac{1-\alpha}{\alpha} \\ G_4(\alpha) = \frac{(1-\alpha)^2}{\alpha^2} \end{cases} \quad (3)$$

In addition, the characteristic length of the Reynolds number is often based on the wire diameter of the mesh, b , and the approach velocity is considered to be either the empty pipe velocity, U_0 , or the velocity through the interstices of the screen, U_0/α .

$$\begin{cases} Re_b = \frac{\rho \cdot U_0 \cdot b}{\mu} \\ Re_{jet,b} = \frac{\rho \cdot U_0 \cdot b}{\mu \cdot \alpha} \end{cases} \quad (4)$$

Using the orthogonal projection of a plain weave wire mesh, the fraction open area of the screen can be easily calculated from geometric measurements according to Eq. (5).

$$\alpha = \left(\frac{M - b}{M} \right)^2 \quad (5)$$

On the other hand, and according to the “flow-through” theory, a friction factor, f , is defined based on a hydraulic diameter, D_h , and void fraction of the screen, ε (not to be confused with the fraction open area, α). While some of these parameters are typically measured experimentally, a method for calculating them theoretically based on screen geometry was presented in the seminal work of Armour and Cannon (1968).

$$f = \frac{\Delta p}{L} \cdot \frac{\varepsilon^2 \cdot D_h}{2 \cdot U_0^2 \cdot \rho} \quad (6)$$

For a plain weave square mesh, Armour and Cannon (1968) defined these parameters according to Equation set (7). The nomenclature was adapted to that of the current work and slightly modified to follow the work of Kołodziej et al. (2012). In these equations, a is the ratio of surface area to unit volume of a screen wire, W is the length of a wire segment, and L is the screen thickness (Armour and Cannon, 1968; Kołodziej et al., 2012).

$$\begin{cases} D_h = \frac{4\varepsilon}{a} \\ \varepsilon = 1 - \left[\frac{\pi}{2L} \cdot \left(\frac{b}{M} \right)^2 \cdot W \right] \\ a = \pi \cdot \frac{W}{M^2} \\ W = \sqrt{b^2 + M^2} \\ L = 2 \cdot b \end{cases} \quad (7)$$

However, in both theoretical approaches (i.e. “flow-through” and “flow-around”) most investigators correlated the pressure losses as a summation of two terms. The first term describes the viscous effects (i.e., laminar flow contribution) and the second term the inertial effects (i.e., turbulent flow contribution). Consequently, as Re becomes large, friction losses, defined as either the friction factor, f , or the ratio $[K_s/G(\alpha)]$, become independent of the flow and assume a constant value. Correlating these losses as a function of Re seems to be the most commonly used approach (Thakur et al., 2003).

$$\text{friction losses} = \{f \text{ or } F(Re)\} \propto \frac{c_1}{Re} + c_2 \quad (8)$$

Variants of this form have also been used to describe pressure drop in other types of static mixers (Thakur et al., 2003) and will also be used in the current study for completeness. This form assumes any exponent of Re , typically, <1 .

$$\text{friction losses} = \{f \text{ or } F(Re)\} \propto \frac{c_3}{Re^{\gamma_1}} + c_4 \quad (9)$$

Recently, a new equation type to correlate the pressure loss coefficient, K_s , was introduced by Brundrett (1993). Through trial and error, the author found that the screen porosity function, $G_2(\alpha)$ was the best to correlate the data along with a new three-component function. $F(Re)$ was based on the wire Reynolds number and had the form shown in Eq. (10).

$$F(Re_b) = \frac{c_7}{Re_b} + \frac{c_8}{\log_{10}(Re_b + 1.25)} + c_9 \log_{10}(Re_b) \quad (10)$$

Brundrett (1993) claimed that the first term on the right-hand side of the equation is dominant at $Re_b < 1$, while the second term which was dubbed as a “blending function” plays a role in the

range $0.1 \leq Re_b \leq 100$. The third term, however, helps reaching a pseudo-constant value for $F(Re_b)$ at large Re_b (>200). Furthermore, the author proved the function to be successful at matching various published experimental data points, the validity of which was later challenged by various authors (Wakeland and Keolian, 2003). This form of dependency on the Reynolds number also became popular in studies investigating pressure drop across screens when used as an insect repellent in greenhouses or screen-houses (Bailey et al., 2003; Teitel et al., 2009; Teitel, 2010; Castellano et al., 2016; Valera et al., 2005).

Other correlations relating the Reynolds number to friction losses also exist in the literature, and these can assume an Ergun equation form. The first to suggest such form were Ingmanson et al. (1961) who proposed the use of the form shown in Eq. (11).

$$f = \frac{c_5}{Re} + \frac{c_6}{Re^{7/2}} \quad (11)$$

This approach was based on the flow-through theory and was later followed by several investigators, like Wu et al. (2005), and Kołodziej and Łojewska (2009), Kołodziej et al. (2009), Kołodziej et al. (2012), though the authors have slightly modified some parameters or employed a different version of Re . It should also be noted that the Ergun equation approach is somewhat more popular in studies where stacks of gauzes were used (Wakeland and Keolian, 2003) where the path of flow is modified and is not as straightforward as it is with single sheets of screens.

2.2. Experimental determination of pressure drop

Most investigators who studied the pressure drop of single-phase flow through plain weave wire meshes did so using gases (e.g., air, N_2 , etc...) or mostly “pure” fluids, (e.g., dehumidified gases or gas-free liquids). These situations remain, however, of little importance for the chemical process industry where most fluids are typically untreated (Azizi and Al Taweel, 2011). The effect of flow velocity on the pressure drop using “real” situations, were previously measured by Chen (1996), El-Ali (2001), Al Taweel et al. (2007), Azizi and Al Taweel (2015), and Abou Hweij and Azizi (2015). In most of these studies and for the new data that is reported here, the effect of flow velocity on the pressure drop was investigated through a tubular reactor/contacter in which several equidistant screens were placed. Depending on the study, the number of screens varied between 6 and 16 and were placed at distances ranging between 10 and 120 mm. This has several advantages over most of the reported data where the experiments were conducted either using one mesh element (Pinker and Herbert, 1967; Kurian and Fransson, 2009; Armour and Cannon, 1968; Ehrhardt, 1983; Bailey et al., 2003), or a large number of tightly packed screens (Kołodziej and Łojewska, 2009; Wu et al., 2005). The current configuration allows a large enough inter-screen distance to ensure that no interaction occurred between the screens, and their large number allows the minimization of the errors that might arise from slight variations in the screen construction. The latter parameter was found by several investigators to give rise to deviations in flow characteristics (Roach, 1987).

All the data used here to correlate the pressure drop with the flow velocity were experimentally obtained using a similar reactor/contacter configuration as schematically depicted in Fig. 2. The inner pipe diameter typically ranged between 21 and 25.4 mm, through which water was metered and pumped to a mixing section equipped with the woven gauzes and the pressure drop across the system was measured using pressure transducers and, in specific studies, using water or mercury manometers. For a more specific description of each experimental setup, the reader is referred to the references mentioned earlier in this section. Furthermore, it should be noted that out of the 212 experimental data

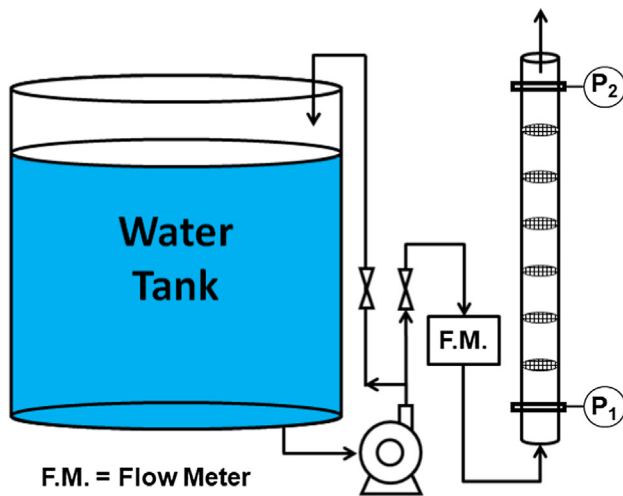


Fig. 2. Schematic representation of the setup used to study the pressure drop through screens.

points used here, 97 measurements (from screens 8 to 13 in Table 1) are reported for the first time and were obtained using the same setup of Abou Hweij and Azizi (2015). In these new studies, and regardless of the screen geometry used, eight woven meshes were placed 60 mm apart in a 25 mm ID pipe, and the pressure drop was measured both at the inlet and outlet of the “reactor/mixer” chamber by means of two pressure transducers (Omega Engineering model PX302-015G). The flow rate was measured by means of a digital flow meter (Omega model: FP7002A) and the overall experimental error was estimated at $\cong \pm 10\%$. The geometry of the various screens that were used is summarized in Table 1.

In summary, the measurements covered screens with open areas ranging between 27 and 73.1% over a Re_b range between 8 and 1683.

2.3. Literature data

To further validate the current experimental results and the methodology, a large set of experimental data was extracted from the open literature. In a similar fashion to various other works, the author relied on transcribing the data from published manuscripts with the aid of a data extraction software. WebPlotDigitizer[®] was used in this case, a software that was proven to be very reliable at extracting data points by digitizing plots (Drevon et al., 2017).

In total more than 800 data points were extracted from the various studies listed in Table 2. The data points considered here all

met the condition of $Re_b > 1$, so the data remains in the same order of magnitude as the experimentally available measurements. In addition, the screen open area in these investigations spanned between 0.21 and 0.84. The estimated error created in the process of data transcription, which was determined by extracting the data more than once, is estimated to be lesser than $\pm 3\%$.

In transcribing the data, the following conditions were always followed:

1. Studies where more than one screen type was employed, only the data for plain-weave square meshes was utilized.
2. Studies where the effect of approach angle was studied, only the experiments where the flow is normal to the screen were considered.
3. Studies that did not consider a dependency on $G(\alpha)$, they either employed the flow-through method, or the data was reported as merely K_s vs. Re_b .
4. Studies shown in Table 2 that considered the flow-through method and still showed a dependency on $G(\alpha)$, they have used both theories to compare their findings,

It should be noted that the data points of Simmons and Cowdrey (1945), Eckert and Pfluger (1942), and Taylor and Davies (1944), were extracted from the work of Annand (1953). The accuracy of this set of data was checked by comparing the data of Schubauer et al. (1950), which were reported by Annand (1953), against the data transcribed from the original report of Schubauer et al. (1950). The match was found to be very good. Also, the data set of Kurian and Fransson (2009) was extracted directly from the graph showing the values of $K_s/G_2(\alpha)$ vs. Re_b because it was not possible to replicate it from the data presented as K_s vs. Re_b . This is because Kurian and Fransson (2000) recalculated the porosity of the screens based on parameters of their experimental setup and no information was presented in their manuscript that would allow rechecking the values.

Furthermore, Annand (1953) and Roach (1987) only presented correlations in their works. That of Annand (1953) was derived by considering 178 data points from previously published data on 22 different gauzes, while Roach (1987) considered data obtained from 17 different studies spanning a broad range of Reynolds numbers.

Other correlations for the “flow-around” approach were found in the literature. These are mainly the result of individual investigators correlating their experimental findings. A list of these correlations that will be used in this work to study the “flow-around” approach along with their expressions is given in Table 3. These correlations are all in terms of $F_2(Re_b) = K_s/G_2(\alpha)$ and applicable for $Re_b > 10$. It should be mentioned that the correlation of Annand (1953) was not explicitly given in his work, but rather

Table 1
Characteristics of the investigated plain weave wire meshes.

Screen Nb.	Mn (-)	M (mm)	b (mm)	α (-)	Re_b (-)	Source
1	24	1.058	0.508	0.27	153–1336	Chen (1996), El-Ali (2001)
2	70	0.362	0.152	0.336	32–293	Al Taweel et al. (2013), Al Taweel et al. (2007), Chen (1996), El-Ali (2001)
3	30	0.845	0.305	0.408	91–588	El-Ali (2001)
4	12	2.117	0.64	0.487	422–1683	Chen (1996)
5	16	1.588	0.23	0.731	152–605	Chen (1996)
6	70	0.363	0.165	0.297	58–370	Azizi and Al (2015), Al Taweel et al. (2007)
7	70	0.364	0.094	0.55	35–81	Al Taweel et al. (2007)
8	20	1.27	0.406	0.462	25–480	New data set and data from (Abou Hweij and Azizi, 2015)
9	20	1.27	0.584	0.291	153–691	New data set
10	30	0.8382	0.3048	0.405	18–550	New data set and data from (Abou Hweij and Azizi, 2015)
11	50	0.508	0.2286	0.3025	14–411	New data set and data from (Abou Hweij and Azizi, 2015)
12	80	0.3175	0.1397	0.3136	8–250	New data set and data from (Abou Hweij and Azizi, 2015)
13	100	0.254	0.1143	0.3025	30–205	New data set

Table 2

Source of the data extracted from the literature.

Source	Extracted Points	$G(\alpha)$	Method
Groth and Johansson (1988)	60	$G_2(\alpha)$	Flow-around
Pinker and Herbert (1967)	49	$G_2(\alpha)$	Flow-around
Eckert and Pfluger (1942)	11	–	–
Taylor and Davies (1944)	14	–	–
Simmons and Cowdrey (1945)	15	–	–
Annand (1953)	–	$G_2(\alpha)$	Flow-around
Roach (1987)	–	$G_2(\alpha)$	Flow-around
Brundrett (1993)	–	$G_2(\alpha)$	Flow-around
Schubauer et al. (1950)	74	–	Flow-around
Ehrhardt (1983)	52	$G_1(\alpha)$	Flow-around
de Vahl Davis (1964)	20	–	Flow-around
Bailey et al. (2003)	52	$G_2(\alpha)$	Flow-around
Wakeland and Keolian (2003)	150	$G_1(\alpha)$ and $G_2(\alpha)$	Flow-around
Kurian and Fransson (2009)	53	$G_2(\alpha)$	Flow-around
Kołodziej et al. (2009)	260	$G_1(\alpha)$	Flow-through
Armour and Cannon (1968)	–	–	Flow-through
Wu et al. (2005)	53	–	Flow-through
Ingmanson et al. (1961)	–	–	Flow-through

Table 3

Various correlations found in the literature.

Authors	$F_2(Re_b) = K_s/G_2(\alpha)$
Annand (1953)	$0.484 + (8.665 \times Re_b^{-0.7847})$
Roach (1987)	$0.52 + (66 \times Re_b^{-4/3})$
Groth and Johansson (1988)	$0.4 + (8.4 \times Re_b^{-4/5})$
Wakeland and Keolian (2003)	$0.4 + (11.5 \times Re_b^{-1})$
Kurian and Fransson (2009)	$0.5 + (26 \times Re_b^{-1})$
Brundrett (1993)	$(7 \times Re_b^{-1}) + (0.9 \times (\log_{10}(Re_b + 1.25))^{-1}) + (0.05 \times \log_{10}(Re_b))$
Bailey et al. (2003)	$(18 \times Re_b^{-1}) + (0.75 \times (\log_{10}(Re_b + 1.25))^{-1}) + (0.055 \times \log_{10}(Re_b))$

tabulated data for $F_2(Re_b)$ vs. Re_b was provided for $20 \leq Re_b \leq 500$. The data was then used to create the best fit ($R^2 = 0.9982$, $SSE = 0.001413$, $RMSE = 0.0108$) shown in Table 3. In addition, Groth and Johansson (1988) did not correlate their data, rather their correlation was provided by Kurian and Fransson (2009) who fitted the measurements of Groth and Johansson (1988). This correlation was also checked against transcribed data from the original manuscript and found to be a true representation.

3. Results and discussion

In this paper, the two approaches of “flow-around” and “flow-through” will be studied and compared. Therefore, this section was divided into two subsections, each of which deals with a different approach. However, the current experimental data measurements will be first presented.

All experimental measurements of pressure drop variation with empty pipe velocity were first plotted in Fig. 3a. It can be discerned that the highest pressure drop corresponded to the screen with the lowest open area (i.e., screen #1), whereas the lowest recorded pressure drop was for the flow through the screen with the largest open area (i.e., screen #5). The rest of the data showed no specific trend with Δp falling between these two limits and no clear distinction based on mesh geometry could be derived. However, when plotted against the wire Reynolds number (cf. Fig. 3b), the pressure drop data became more stratified, and groups of screens became distinguishable. It was interesting to note that five different groups could be differentiated. The first group is formed of screens number 2, 6, 7, 12, and 13, the second is made of screen number 11, the third includes screens number 1, 3, and 10, the fourth com-

prises of screens number 5, 8, and 9, while screen number 4 constituted the fifth group. What is to note is that while the pressure drop data is plotted against the wire Reynolds number, it is the screen mesh size, M , that was found to play the major role in stratifying the results. No other common denominator was found (e.g., α , b , M - b). The first group has the lowest values of M ($M < 0.365$ mm), while the second had an intermediate mesh size, $M = 0.508$. The third group showed average mesh sizes with $0.83 < M < 1.06$, followed by the fourth where $1.27 < M < 1.59$. Finally, the fifth group had the largest value of $M = 2.117$ mm.

3.1. Flow-around approach

Following the “flow-around” approach, all measurements were analyzed in terms of the pressure loss coefficient which was plotted against the wire Reynolds number in Fig. 4. In a similar fashion to all published data, the pressure loss coefficient decreased with an increase in the flow velocity until it assumed a constant value at large Re_b . It can be clearly discerned that the highest and lowest values of the loss coefficient also corresponded to the screens with the lowest and largest fraction open areas (i.e., $\alpha = 0.27$ and 0.73 or screens # 1 and 5), respectively. Another observation was noted, whereas, with the exception of screen #3, all meshes with open areas between 0.29 and 0.34 showed a similar behavior with their loss coefficients being very close to each other and fell in the same region on the plot. Also, Screen #6 shows an apparent increase in the value of K_s at higher Re_b . This is an erroneous trend that can be attributed to experimental errors since these changes in the value of K_s correspond to $\approx \pm 4\%$ relative error in its value over the last five measurements.

3.1.1. Effect of $G(\alpha)$

In the study of pressure drop of flows across a woven wire mesh, a major contradiction that can be found in the literature is

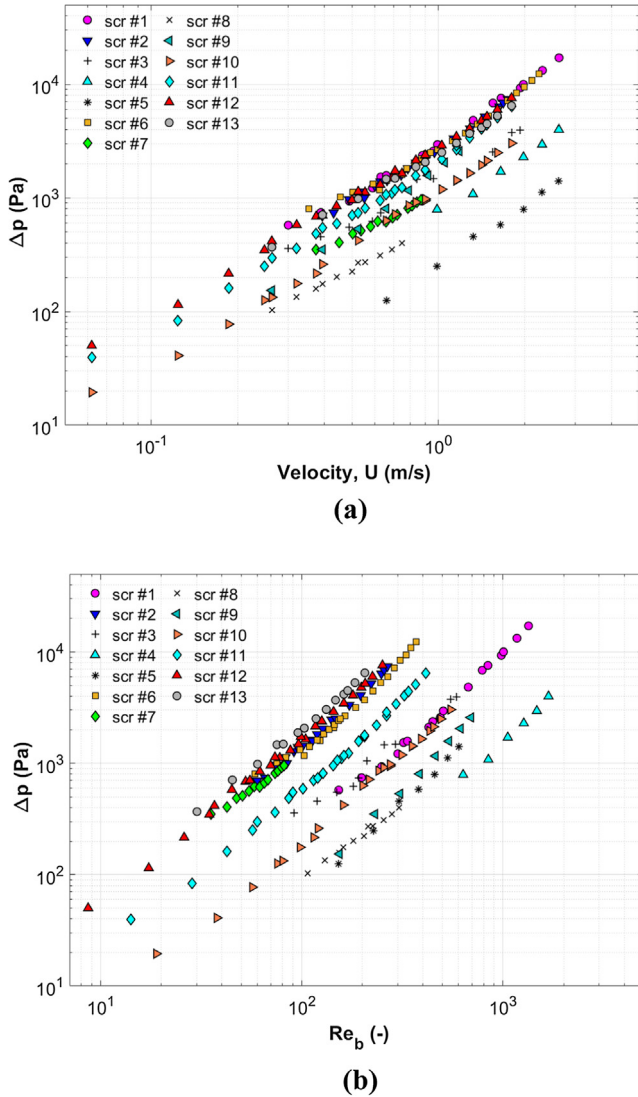


Fig. 3. Variation of the pressure drop with (a) the empty pipe velocity, and (b) Re_b .

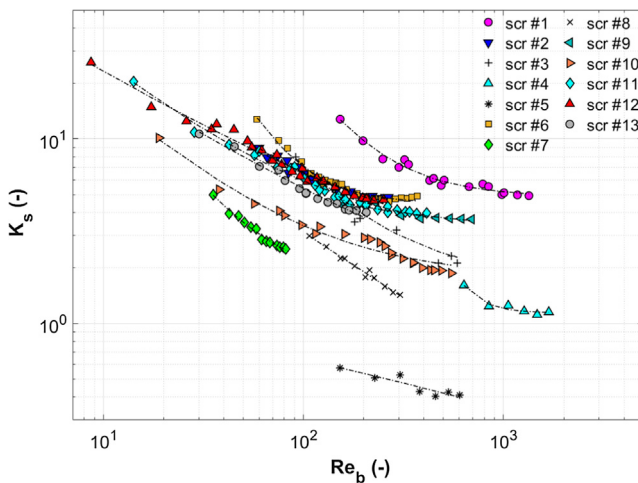


Fig. 4. Variation of the screen pressure loss coefficient, K_s , with the wire Reynolds number, Re_b , for all screens listed in Table 1.

the form of $G(\alpha)$. As can be seen from Table 2, no agreement exists on that matter. For this purpose, the current experimental data were first analyzed in terms of varying $G(\alpha)$ to check for its effect. The variation of $K_s/G(\alpha)$ with the wire Reynolds number for the various forms of $G(\alpha)$ is plotted in Fig. 5 against the respective best fit line. This line was selected in the form of Eq. (9). As such, it was interesting to note that while the best R^2 value was obtained for $K_s/G_3(\alpha)$, the function $G_2(\alpha)$ showed a better global fit with lower SSE and RMSE values where lesser overall scatter was observed. The fit was also conducted using the form shown in Eq. (8), and similar trends were also detected. Consequently, the analysis of the current data will continue using only $G_2(\alpha)$.

For a clearer perspective, the variation of, $F_2(Re_b) = K_s/G_2(\alpha)$, with changes in the wire Reynolds number, Re_b , were plotted in Fig. 6. The data depicts the known trend of decreasing $F_2(Re_b)$ with an increase in Re_b and that all points collapse on the same curve. Only a few outliers, notably Screen #7 and some measurements of Screen #3, can be observed to fall outside the general trend.

3.1.2. Comparison with literature data

The data points extracted from the literature were all normalized and recomputed based on the reported screen geometry parameters to convert their values to the form $F_2(\alpha) = K_s/G_2(\alpha)$. This data was then plotted against the corresponding wire Reynolds number, Re_b , in Fig. 7a. All the data exhibited the same trend of decreasing $F_2(\alpha)$ with an increase in Re_b ; however, a decent spread could be observed. It should be noted that, except the data set of Pinker and Herbert (1967), most of the data points fell in the range of $Re_b < 900$ and their general trend seemed to decrease continuously and start to plateau at or slightly beyond $Re_b = 300$.

The constant value of $F_2(\alpha)$ at high Re_b was also fluctuating between the various literature sources. While it is not readily discernable from Fig. 7, this data fluctuated between 0.4 and 0.63. Only the data of Kołodziej et al. (2009) seems to plateau at the highest value of ~ 1 . However, it was only Pinker and Herbert (1967) who measured the pressure losses at $Re_b \geq 1000$, with the rest of the experiments conducted at $Re_b < 900$.

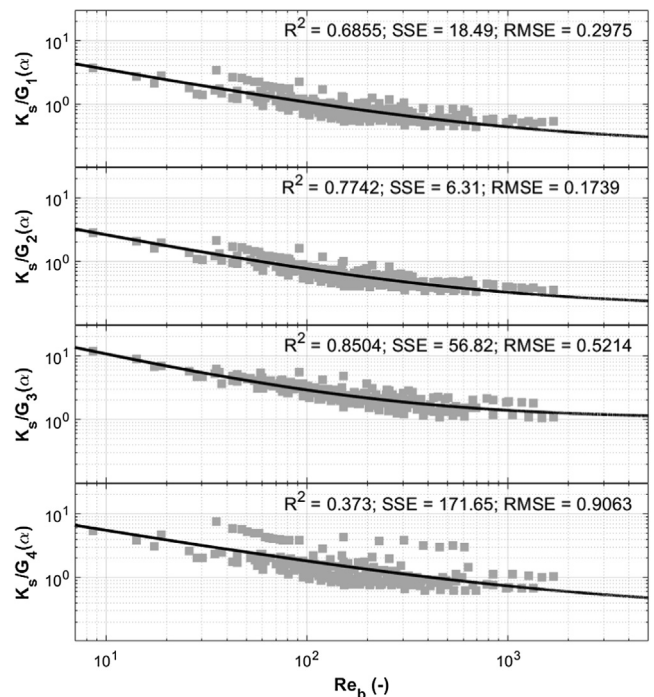


Fig. 5. Variation of $K_s/G(\alpha)$ with Re_b for the various forms of $G(\alpha)$.

This behavior becomes more evident when one compares the experimental data sets with the literature correlations as plotted

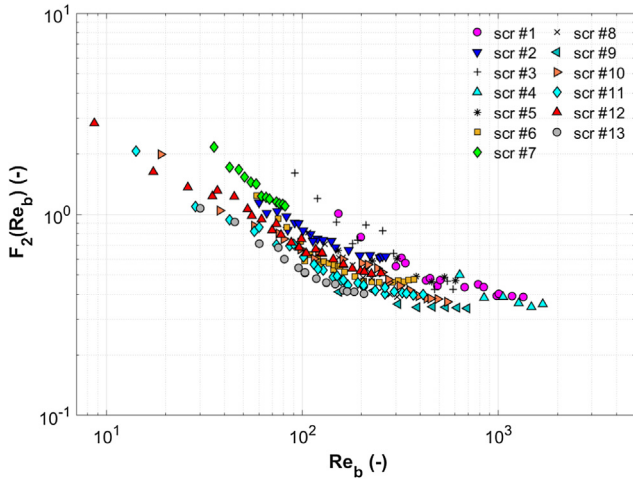


Fig. 6. Variation of $F_2(Re_b)$ vs. Re_b for all screens listed in Table 1.

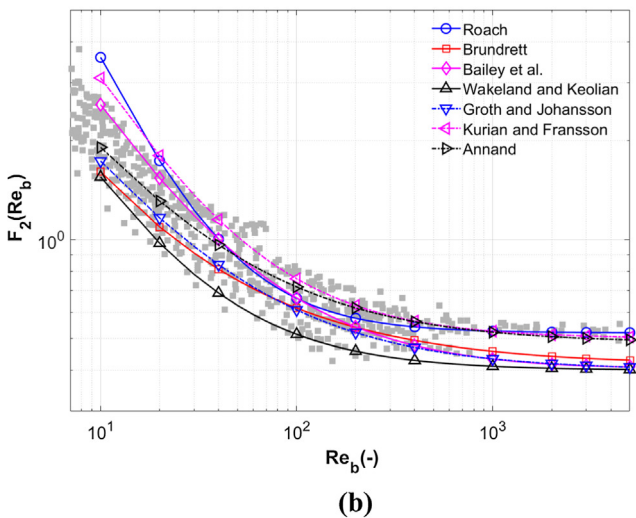
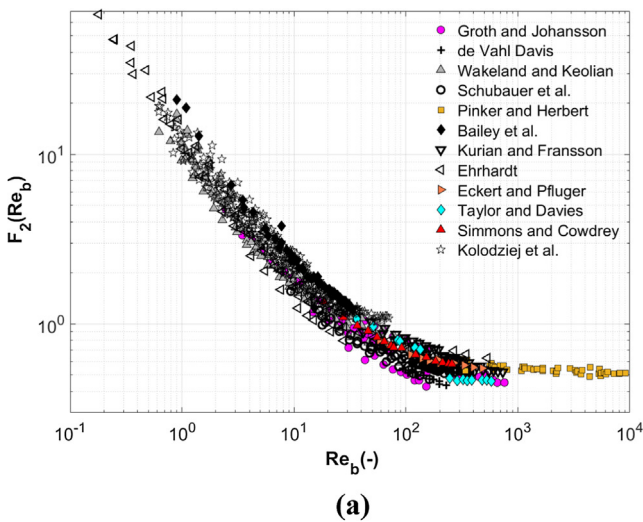


Fig. 7. Variation of $F_2(Re_b)$ with the wire Reynolds number (a) for the data extracted from the literature, and (b) comparison between the literature data (grayed) and literature correlations.

in Fig. 7b. The correlations were plotted for a Reynolds number in the range $10 \leq Re_b \leq 5,000$. Even though this might fall outside the developed limits for some, it was regarded as an extrapolation to check the overall tendency of the equations.

It is clear from Fig. 7b that the correlations span the entire width of the literature data scatter. However, no single correlation showed an above average trend, with most of them showing a good fit in a particular region, but weaker in another. Only the correlation of Wakeland and Keolian (2003) predicted values that are consistently lower than the majority of the experimental data. It should be noted that Wakeland and Keolian (2003), who provided their own correlation shown in Table 3, argued that in order to obtain a good fit for the data, the pressure loss coefficient, K_s , should be normalized using the function $G_1(\alpha)$ rather than $G_2(\alpha)$. Furthermore, the correlation of Roach (1987), which seems to describe fairly well the data for $Re_b > 40$ fails to be extrapolated to smaller values. In fact, Roach (1987) presented two correlations, one for $Re_b < 10$ and the second for $Re_b > 40$, but only the latter was adopted here. This is because the former expression follows a linear relationship that correlates with Re^{-1} and its extrapolation would render a straight line with values that are very small. Similarly, the correlations of Brundrett (1993) and Bailey et al. (2003) predicted much smaller values for $Re_b > 1000$ than those measured mainly by Pinker and Herbert (1967). As a matter of fact, for large values of $Re_b (>1000)$, the seven correlations segregated into two distinct groups differing by the value at which they plateau. The first group formed by the correlations of Annand, Kurian and Fransson, and Roach, predicted constant values of $F_2(\alpha)$ that are closer to (albeit slightly lower than) those measured by Pinker and Herbert (1967) and in the range of 0.5, whereas the second group that was formed by the other investigators, predicted a constant value of around 0.4 for $Re_b > 1000$.

Finally, the current experimental measurements were compared with the data extracted from the literature. This set was plotted in Fig. 8 as $F_2(\alpha)$ vs. Re_b . It can be discerned that the current measurements do not deviate a lot from the data reported in the literature and it is very close to it. With the exception of two screens (i.e., screens # 7 and 9), all the data fell within the upper and lower envelopes of the literature data (i.e., dashed lines in Fig. 8). It can also be observed that some experimental measurements decrease at a slightly steeper slope when compared to the data from literature. This could be attributed to the fact that “real” working fluids were used in these experiments whereby filtered

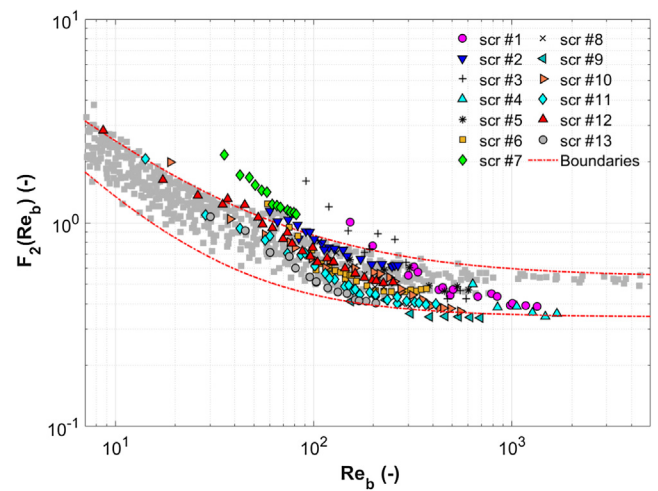


Fig. 8. Variation of the experimental data in terms of $F_2(\alpha)$ vs. Re_b for both literature data (grayed out) and current experimental results. The dashed lines are the upper and lower envelopes of the literature data.

tap water was employed. This is in contrast with all the literature data reported here where air was used as the working fluid. Similarly to Ehrhardt (1983), the formation of microbubbles was observed at lower velocities in various experiments. This is because water was not degasified prior to the experiment. The formation of these bubbles increases the pressure drop across the screen and causes the slope of $F_2(Re_b)$ vs. Re_b to become slightly steeper. Furthermore, the presence of air bubbles affects the wettability of the stainless-steel woven mesh because the latter has a higher affinity to air than water. Because of their low volume fraction, this contributes to a slight increase in the pressure drop. However, the wettability effect was deemed negligible because the capillary number was always much larger than the minimum value of 10^{-5} (by at least two orders of magnitude) and the volume fraction of these bubbles is very small. It should also be added that similarly to the observations of Ehrhardt (1983), these bubbles detach from the screen after a certain minimum flow velocity has been reached, beyond which no bubbles would be retained. The value of this threshold velocity is however dependent on the screen geometry and its determination would require a detailed analysis that is beyond the scope of the current work.

3.1.3. Correlating the results

An attempt to correlate the data was undertaken. To overcome the pitfall whereby a correlation based on the current experimental data only would have limited applicability and validity, it was decided to use the complete set of data obtained from current experiments and literature data (cf. Table 2). In total, 957 data points corresponding to Re_b ranging between 2 and 14,000 were used. In addition, the various correlation forms presented earlier were employed, and the best fit was obtained using Eq. (12) ($R^2 = 0.9318$), with the fit shown in Fig. 9a.

$$F_2(Re_b) = \frac{10.76}{Re_b^{0.8213}} + 0.4537 \quad (12)$$

It can be clearly seen that the correlation line appears to be an excellent representation of the data as shown in Fig. 9a where most of the data fall within $\pm 30\%$ of its predictions. The slight under-prediction that it shows against the data of Pinker and Herbert (1967) at large Re_b , however, is still in line with other findings in the literature which report a “plateau” at values ranging between 0.4 and 0.52 (Groth and Johansson, 1988; Wakeland and Keolian, 2003). For example, Groth and Johansson reported a value of 0.45 at $Re_b \approx 820$.

Furthermore, when compared to the correlations from the literature in Fig. 9b, the proposed correlation falls inside the upper and lower bounds formed by the various correlations. Fig. 10a shows the pressure drop predictions using Eq. (12) plotted against the experimentally measured data (of the current work). It can be seen from the parity plot that all predictions fall within $\pm 30\%$ of the measured values with a mean relative error of 20.8%.

A multi-linear regression was also performed on the pressure drop data to correlate it against the major screen geometric characteristics (i.e., b , M , α) as well as the flow velocity, U . This would serve as an attempt to check the comprehensiveness of the flow approach whereby the pressure drop coefficient, K_s , that has been normalized by the fraction open area of the screen, is correlated using only the wire Reynolds number, Re_b . The best fit of the current experimental data was obtained using the form presented in Eq. (13) with $R^2 = 0.971$.

$$\Delta p = 817.63 \cdot b^{0.609} \cdot M^{-0.96} \cdot \alpha^{-1.155} \cdot U^{1.576} \quad (13)$$

The pressure drop predictions obtained using this multi-linear regression approach (Eq. (13)) are compared together with the predictions obtained using the flow-around approach against the

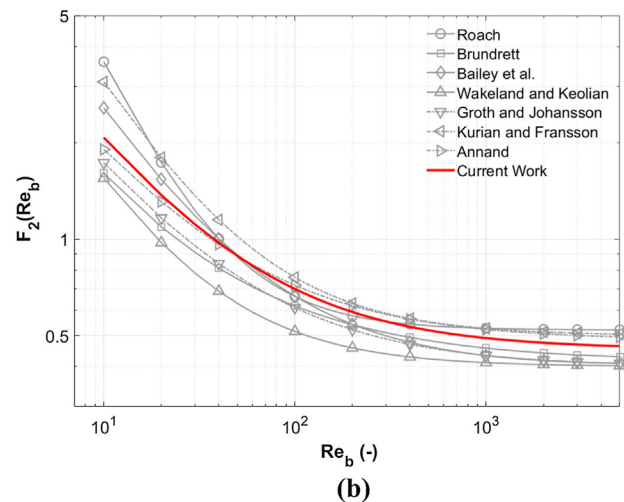
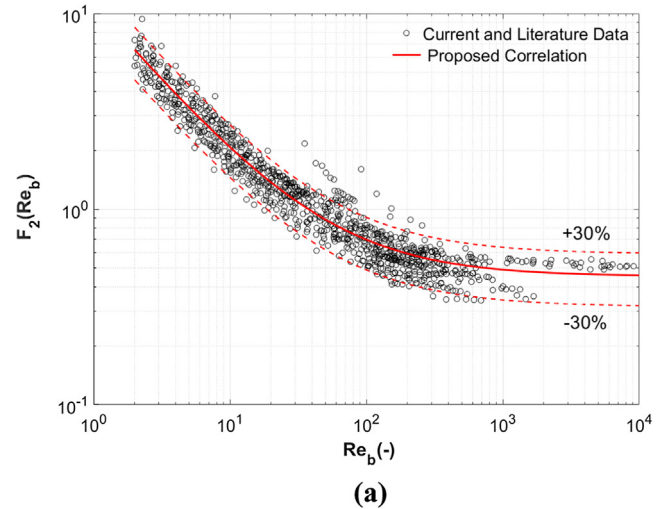


Fig. 9. Best fit of all data points using the correlation presented in Eq. (2); (a) correlation versus experimental measurements, (b) correlation versus literature correlations.

experimental measurements in Fig. 10b. It is clear that both approaches predict relatively close results with those obtained using the multi-linear regression showing relatively less scatter. To better compare these two approaches, their predictions were plotted against each other in Fig. 10c. While the predictions appear to be very close, a mean relative error of 13% was calculated with the multi-linear regression model underpredicting the values calculated using the flow-around correlation for lower Δp , but overpredicting them towards the higher end of pressure drop.

It should be noted that the use of Re_b in lieu of the flow velocity, U , would have resulted in the same correlation with the only difference being the exponent of the wire diameter, b .

3.2. Flow-through approach

As previously mentioned, the “flow-through” approach considers the flow of fluids through a woven mesh as being analogous to flow through a packed bed. Similarly, to the discrepancies between the various approaches to calculate the pressure drop using the “flow-around” theory (i.e., various forms of $G(\alpha)$), there exist two major approaches to calculating Δp using the “flow-through” model. The first relies on treating the woven mesh as a bundle of tangled tubes, while the second assumes the mesh to be equivalent

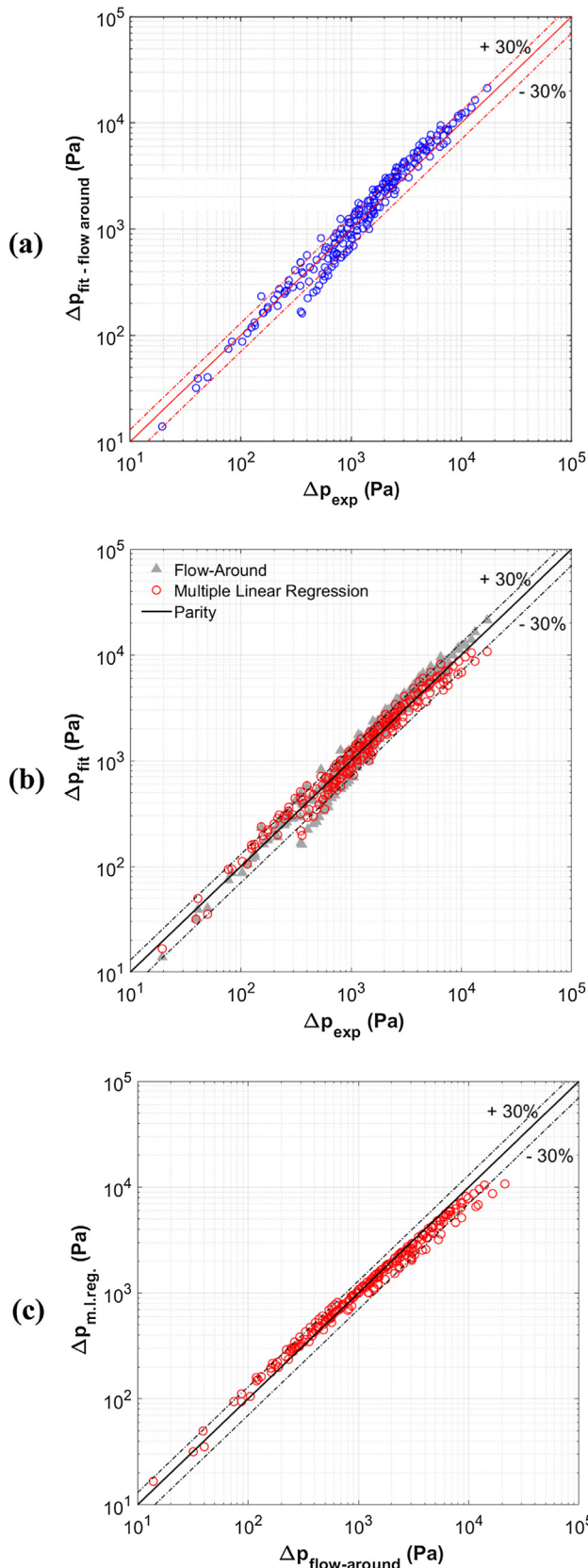


Fig. 10. Parity plots for the various approaches. (a) predictions of the flow-around approach plotted against experimental measurements; (b) predictions using the multiple linear regression are plotted along predictions of Eq. (12); (c) both predictions plotted against each other.

to a number of submerged spherical particles (Wu et al., 2005; Kołodziej et al., 2009; Kołodziej et al., 2012). Consequently, the pressure drop would become the summation of resistances in either one of these methods, and calculating it would, therefore, rely on applying a variant of the Ergun equation (Ergun, 1952) to the system.

In this paper, only the first approach that considers the screen as a bundle of tubes will be considered. However, a reference to some other works which used a different methodology will be given, highlighted, and compared to this work.

In this approach, the Fanning friction factor is defined according to Eq. (6), and the Reynolds number also depends on the theoretical approach because the utilized characteristic length follows the assumed geometric model. Following the bundle of tubes approach, the Reynolds number is typically calculated based on the hydraulic diameter, D_h , whereas it would rely on the equivalent sphere diameter, D_s , if the model of submerged spheres was selected. It should be noted, however, that these diameters, and consequently their corresponding Re , remain related to each other. Eq. (14) shows the values of the various diameters and their corresponding Re following the works of Kołodziej et al. (2012) and Wu et al. (2005).

$$D_h = 4 \frac{\varepsilon}{a} \rightarrow Re_h = \frac{\rho \cdot U_0 \cdot D_h \cdot \tau}{\mu \cdot \varepsilon}$$

$$D_s = 6 \left(\frac{1-\varepsilon}{a} \right) \rightarrow Re_s = \frac{\rho \cdot U_0 \cdot D_s \cdot (1-\varepsilon)}{\mu}$$
(14)

where τ is a tortuosity factor ($\tau = 1 + [(1 - \varepsilon)/2]$) following the work of Carman (1956) and utilized by Kołodziej and Łojewska (2009) who employed the hydraulic diameter approach. However, the two Reynolds numbers can be related to each other through the mesh geometric parameters, whereby after some mathematical manipulation the relationship between the two can be derived.

$$Re_h = \frac{Re_s}{(3/2)(1 - \varepsilon)^2}$$
(15)

Following the definition of the Fanning friction factor and Reynolds number based on the bundle of tubes approach, the current experimental data was converted and plotted in Fig. 11. This figure shows a decreasing friction factor with an increase in Re_h . This trend is in line with all reported data in the literature. Furthermore, it can be discerned that except Screen #7 all the data almost fall on the same curve which reaches an asymptotic value for $0.2 < f < 0.3$.

It should be noted that in order to perform these calculations, the various required geometric parameters were calculated

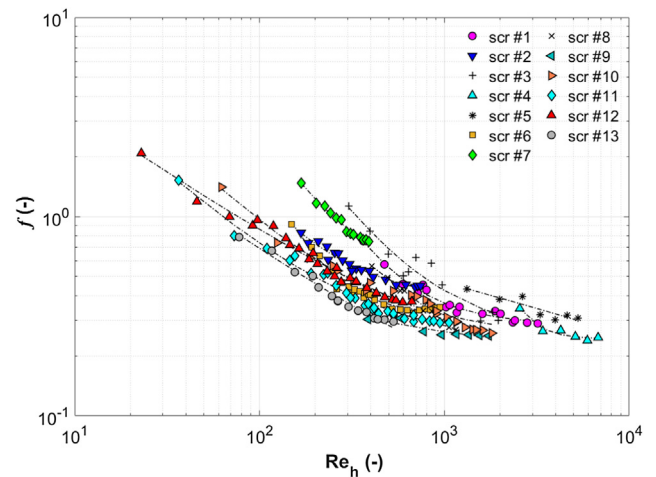


Fig. 11. Fanning friction factor derived from current experiments plotted against the Reynolds number.

following the theoretical equations presented by Armour and Cannon (Armour and Cannon, 1968) and listed in Equation set (7).

3.2.1. Comparison with literature data

In order to test the validity of the experimental measurements in the “flow-through” approach, the measurements were compared against data reported in the literature. It should be noted that many investigators employed the “flow-through” approach to studying the pressure drop across a woven mesh (cf. Table 2). However, almost each one of them has employed a different definition for Re and f . Our current approach closely follows the works of Kołodziej and Łojewska (2009) and Kołodziej et al. (2012), and therefore it was easiest first to compare the measurements to their original data set reported in (Kołodziej et al., 2009). In that work, original measurements for the pressure drop across woven and knitted meshes were reported, and therefore only the woven mesh data was extracted for this purpose. Fig. 12a shows this comparison where it is clear that the data appear to fall on the same curve. However, the current measurements appear to have a lower friction factor than that reported by Kołodziej et al. (2009). As previously mentioned, the current data set plateaus at $0.2 < f < 0.3$, whereas that in (Kołodziej et al., 2009) reaches an asymptotic value of $0.56 < f < 0.62$. It is worth mentioning that these asymptotic values of Kołodziej et al. (2009) were obtained from extrapolation of data measured at low Re_h (< 300). This is in contrast with the current data set that was measured at values of Re_h ranging between 27 and 7600.

In an attempt to better explain these observations, other sets of data reported in the literature were also used. For this purpose, various literature data that were published under the “flow-around” approach were recalculated and converted to the “flow-through” approach. Namely, the data sets of Groth and Johansson (1988), de Vahl Davis (1964), Schubauer et al. (1950), Kurian and Fransson (2009), Wakeland and Keolian (2003), Ehrhardt (1983), Wu et al. (2005), and Armour and Cannon (1968), were used. In total 462 data points were converted from their original values to fit the approach adopted in this section.

With the exception of the data of Armour and Cannon (1968) and Wu et al. (2005), the data sets were converted to the flow-through approach by performing all necessary calculations based on screen geometry parameters reported in the manuscripts (i.e. α , b , M , etc. . .) and using Eq. (7) and the transcribed data. The data set of Armour and Cannon (1968) proved tricky to extract from the original work since differentiating between the various plain woven screens was not possible in their original manuscript, and therefore the 22 data points used here and attributed to them were extracted from their correlation as presented by Kołodziej and Łojewska (2009) who converted it to fit the current bundle-of-tubes model. These data points spanned the Re_h range between 2 and 220. Wu et al. (2005) also measured the pressure drop of flow through woven screens. However, they reported the data following the submerged spherical particles approach. For this reason, their data had to be converted to the bundle-of-tubes approach. While the Reynolds number conversion was previously presented in Eq. (14), their friction factor also had to be converted following a mathematical manipulation, the result of which is shown in Eq. (16).

$$f_{wu} = \frac{\Delta p}{L} \cdot \frac{D_s}{\rho U_0^2} \cdot \frac{\varepsilon^3}{1 - \varepsilon} = 3f \quad (16)$$

Fig. 12b clearly shows how the various data from the literature compare against each other. It can be easily discerned that all data points fall on the same curve and that the asymptotic value at high Re is much closer to the current experimental measurements as opposed to that of Kołodziej et al. (2009). One outlier is the data

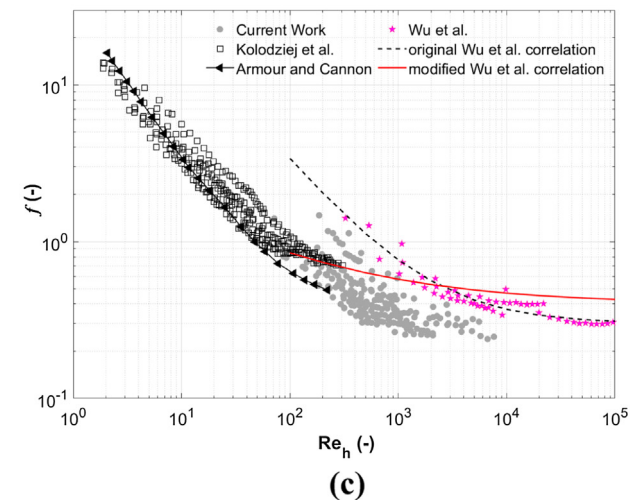
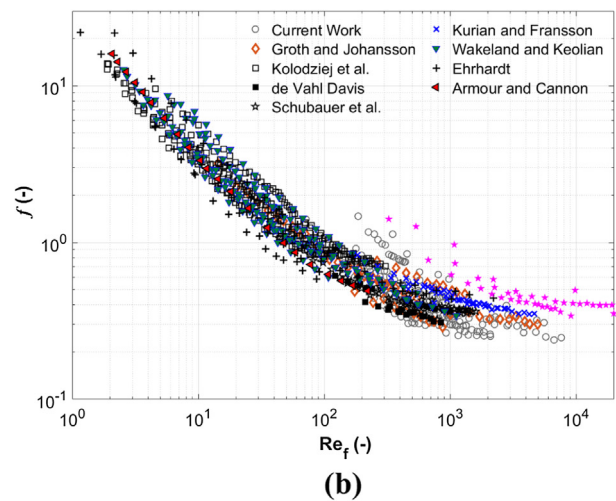
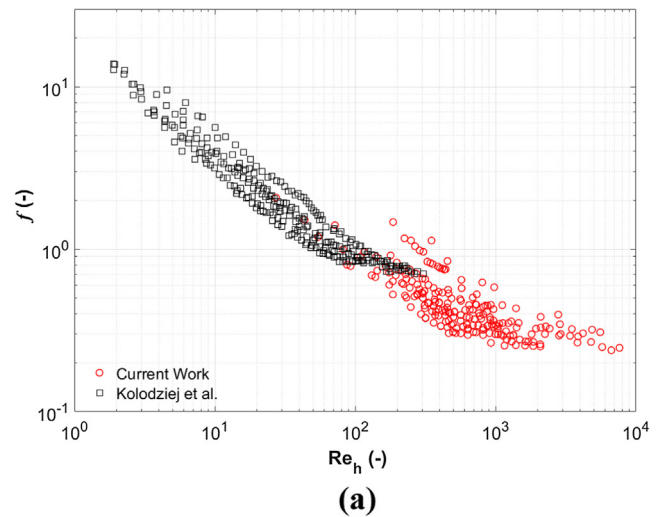


Fig. 12. Comparison of the current measurements to data from the literature. (a) comparison with the data of Kołodziej et al. (2009), only; (b) comparison with data extracted from various sources; (c) highlighting Wu et al. (2005) data and correlation.

set of Wu et al. (2005) that shows values of the friction factor that are much higher than most of the reported data. This observation is in line with that of Kołodziej et al. (2009) who, in an attempt to

compare their experimental measurements with literature data, reported that the correlation of Wu et al. (2005) rendered higher predictions than their observed values. To better explain their data, Kołodziej et al. (2009) modified the correlation of Wu et al. (2005) and proposed a new form for it. This correlation is plotted in Fig. 12c, for $Re_h > 100$ with many other data points removed from the plot to reduce the clutter, and it highlights the danger of extrapolating results based on a small Re range. It should also be mentioned that while the data of Wu et al. (2005) reached values of $Re_h \cong 100,000$, Fig. 12b focused only on a reduced range of Re_h up to 20,000. The full range of data is shown; however, in Fig. 12c along with the original correlation that they proposed.

3.2.2. Comparison with analytical models

Because the “flow-through” approach is based on the Ergun equation (Ergun, 1952), several models that adapted this equation to flow through woven meshes are available in the literature (Armour and Cannon, 1968; Kołodziej and Łojewska, 2009; Wu et al., 2005; Ingmanson et al., 1961). Notably, the model developed by Kołodziej and Łojewska (2009) appears to have been thoroughly refined where theories from flow through porous media were used to calculate the effective flow length and the effective velocity (Bussi ere et al., 2017).

According to Kołodziej and Łojewska (2009), the pressure drop across a woven wire mesh results from the contribution of both the laminar and turbulent components which follow a Darcy-Weisbach type equation (Kołodziej et al., 2012; Kołodziej and Łojewska, 2009) as shown in Eq. (17).

$$\Delta p = \Delta p_L + \Delta p_T = 4(f_L + f_T) \cdot \frac{\rho U_e^2}{2} \cdot \frac{L_e}{D_h} \tag{17}$$

where U_e is the effective flow velocity, and L_e is the effective length of the bed. However, by analogy with the flow through porous media, Kołodziej and Łojewska (2009) also considered that the flow would be deflected by a certain angle, θ , and would follow a tortuous path defined by a tortuosity, τ . The deflection angle is that formed between the direction of the flow inside the porous medium and the direction given by the thickness of the crossed porous medium (Bussi ere et al., 2017). Accordingly, the various parameters can be calculated following the set of equations presented as Eq. (18).

$$\begin{cases} U_e = \frac{U_0 \cdot \tau}{\varepsilon} \\ L_e = \frac{L}{\cos(\theta)} \\ \tan\theta = \frac{b}{2(L-b)} \end{cases} \tag{18}$$

Furthermore, the laminar component was considered by analogy to a laminar flow developing in a very short channel. Accordingly it can be calculated following Eq. (19).

$$f_L \cdot Re_h = \frac{3.44}{\sqrt{L^+}} + \frac{\frac{1.25}{4L^+} + 16 - \frac{3.44}{\sqrt{L^+}}}{1 + [0.00021/(L^+)^2]} \tag{19}$$

where L^+ is the hydraulic dimensionless channel length ($L^+ = b/(D_h \cdot Re_e)$). Similarly, the turbulent component followed the Blasius equation for smooth pipes and is described in Eq. (20).

$$f_T = \frac{0.0791}{Re_h^{0.25}} \tag{20}$$

Accordingly, the pressure drop across a woven mesh can be calculated using Eq. (21).

$$\begin{aligned} \frac{\Delta p}{L} &= 4(f_L + f_T) \frac{\rho U_0^2}{2\varepsilon^2} \frac{1}{D_h} \frac{\tau^2}{\cos(\theta)} \\ &= 4(f_L + f_T) \frac{\rho U_0^2}{2b} \frac{(1 - \varepsilon)}{\varepsilon^3} \frac{\tau^2}{\cos(\theta)} \end{aligned} \tag{21}$$

The description of the model of Kołodziej and Łojewska (2009) presented here followed the nomenclature presented by Kołodziej et al. (2012). It should be noted that according to Eq. (18), the angle θ would be constant for all plain square woven meshes. However, another definition was originally proposed by Kołodziej and Łojewska (2009) in which it was defined as $\tan\theta = b/M$.

Accordingly, this model was solved and the pressure drop predictions were compared to the current experimental measurements in Fig. 13a. It can be clearly seen that the majority of the experimental measurements fall within $\pm 30\%$ of the model predictions. The average relative error was found to be 24% with the majority of the data being underpredicted by the model. The goodness of fit was calculated as $R^2 = 0.7186$. While the experimental measurements were conducted under non-ideal conditions, and a measurement error of $\sim 10\%$ is expected, it is believed that the large discrepancy between the model and experimental data could

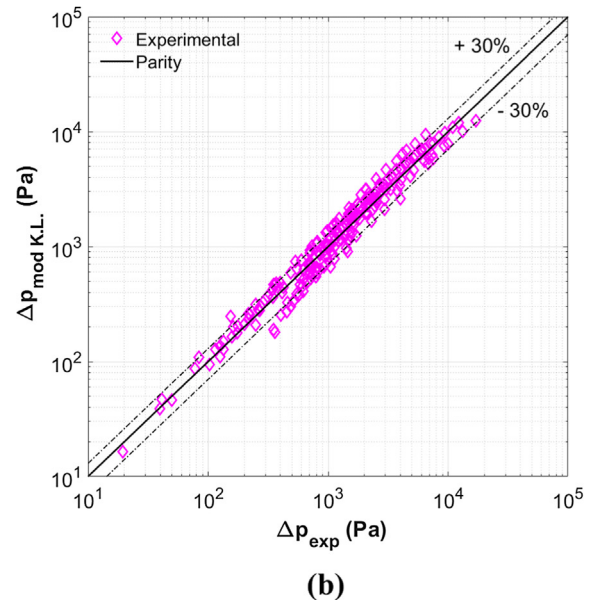
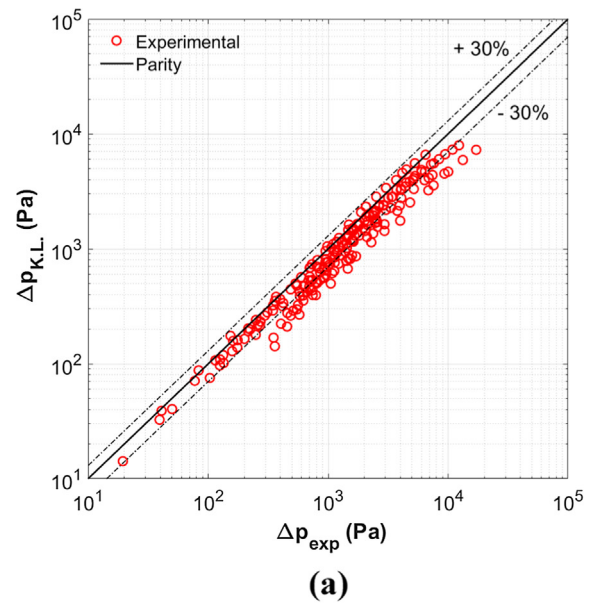


Fig. 13. Parity plot showing the fit between the experimental measurements and the predictions of (a) the model of Kołodziej and Łojewska (2009), and; (b) the modified model using Eq. (22).

also be attributed to the oversimplification of the turbulent component. While the use of a Blasius-type equation has been employed to describe the turbulent component of the pressure drop across various static mixers (different than woven meshes) (Theron and Le Sauze, 2011; Li et al., 1997), it is proposed that this component be modified to fit the experimental observations better. Consequently, it was found that Eq. (20) needed to be multiplied by a factor of 6.44 in order to better fit the current experimental data ($R^2 = 0.916$) at a much lower relative error of 9.37%, without altering the dependency on the Reynolds number. The form of the modified turbulent component of friction is shown in Eq. (22) and the fit in Fig. 13b. This is expected to apply when the measurements are conducted at higher Re_h where the turbulent component plays a significant role.

$$f_T = \frac{0.509}{Re^{0.25}} \quad (22)$$

3.2.3. Correlating the results

An attempt to correlate the data was also undertaken for the “flow-through” approach. Following the same methodology applied for the “flow-around” approach, all literature data was employed in generating the best fit correlation. All the data points presented in Fig. 12b were used with the exception of the data of Wu et al. (2005) since it appeared to show larger values of f compared to the other data sets. In total 865 data points corresponding to Re_h ranging between 2 and 7630 were employed. Similarly to the previous approach, the best fit ($R^2 = 0.9537$) was obtained using the form presented in Eq. (9), with the various parameters shown in Eq. (23).

$$f = \frac{22.97}{Re_h^{0.8011}} + 0.3079 \quad (23)$$

Fig. 14a clearly shows that this correlation line is a good fit to all the data points, where it cuts them through the center with most of the data falling within $\pm 30\%$ from it. It is interesting to note that this fit line is capable of closely predicting the measurements of Wu et al. (2005) for the very high Re_h ($>20,000$). Fig. 14b also shows how the fit compares with various correlations from the literature. The correlations of Armour and Cannon (1968), Wieghardt (1953), and Ingmanson et al. (1961) were extracted from Kołodziej et al. (2012) and extrapolated to fit the more extended range of $Re_h < 20,000$. Except the correlation of Wieghardt (1953) that is clearly out of range for $Re_h > 1000$, the best fit line predicts lower f values than all other correlations. However, that of Wu et al. (2005) seems to overlap with the current fit line at $Re_h > 20,000$.

Using this proposed correlation, the predicted pressure drop was plotted against the experimentally measured points in Fig. 15. This parity plot clearly shows that the majority of the data fall within $\pm 30\%$ of the predictions with a mean relative error of 21%.

3.3. Comparing the two approaches

The two approaches of “flow-around” and “flow-through” were then compared against each other. For this reason, the pressure drop predictions of the current experimental measurements obtained from both correlations (cf. Eqs. (12) and (23)) were plotted together on a parity plot. Fig. 16a shows how the two predictions compare against each other where it is clear that both correlations render similar results. This is further confirmed in Fig. 16b where the predictions of both correlations were plotted against each other, and the graph shows an almost perfect fit with the parity line ($R^2 = 0.9998$) and an average relative error of 3.4%. It should be noted that both correlations showed a similar depen-

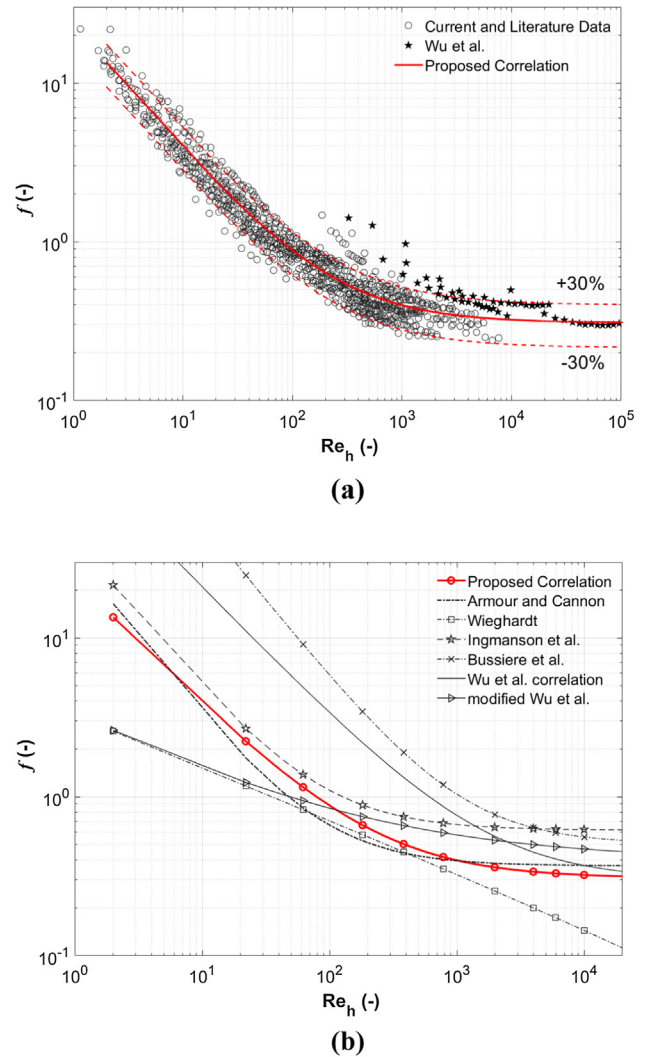


Fig. 14. Best fit of all data points using the correlation presented in Eq. (23). (a) fit vs. experimental data from literature; (b) fit vs. various correlations from literature.

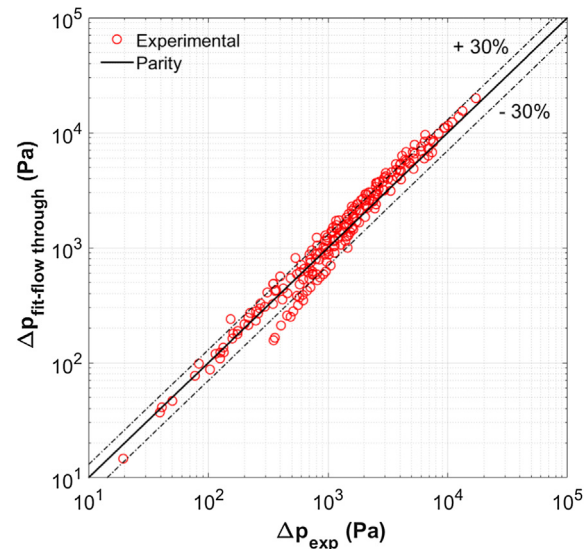
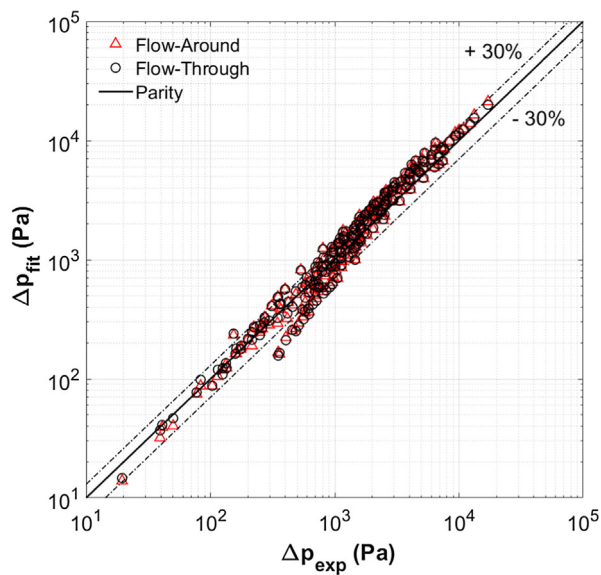
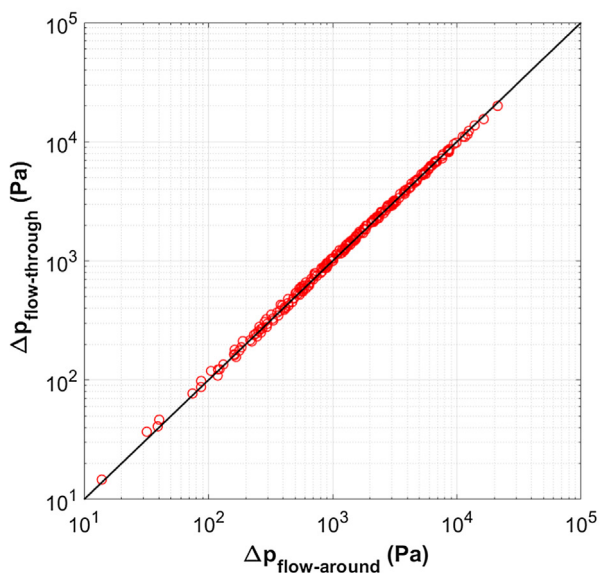


Fig. 15. Parity plot showing the fit between the experimental measurements and the predictions of Eq. (23).



(a)



(b)

Fig. 16. Parity plots comparing the two theoretical approaches. (a) predictions plotted against experimental measurements; (b) predictions plotted against each other.

dependency on the Reynolds number (≈ -0.8) while they were derived using slightly different data sets.

Because the two models, flow-around and flow-through, rendered similar predictions, comparing the flow-through approach to the multi-linear regression (Eq. (13)) was omitted as it would render results similar to those presented in Section 3.1.3.

4. Conclusion

The pressure drop of fluids across plain woven wire screen meshes in circular tubes was investigated in this work. In total, 212 experimental data points obtained under “real” conditions, were examined. This is in contrast to most of the experiments reported in the literature where mostly “ideal” fluids and/or conditions were employed (e.g., moisture-free gases, degasified liquids,

flat velocity profiles, etc...). To further the analysis, >800 data points were extracted from the literature and compared to the current data set.

Furthermore, the analysis was conducted according to the two main theories in the field, namely, the flow-around and the flow-through approaches. It was found that the current measurements match the literature data obtained using “ideal” conditions, although certain minor deviations appear. However, one should note that analyzing more than 1000 data points showed that regardless of the approach, the measurements will always fall on the same curve, the scatter of which is wide and can reach $\pm 50\%$. One should note that due to the delicate nature of finely woven meshes, any slight modification to the screen geometry (e.g., a tweaked wire, wire roughness, etc...) can have a significant effect on the measured pressure drop.

All the collected and measured data were then used to develop general correlations for predicting the pressure loss coefficient, K_s , and the Fanning friction factor, f . It was shown that no matter which approach is used, both theories will lead to similar predictions.

The trendlines that were developed in the current work were found to better describe the various measurements than all correlations available in the literature because of the large number of data points used to derive them. Unlike previous studies where investigators looked at their own specific data over a limited range of Reynolds numbers using a small number of screens, the current analysis covered more than 60 different plain square woven meshes, with data obtained over a large spectrum of Re . However, one should always expect a deviation of about $\pm 30\%$ from predictions. Such deviations between measurements and predictions should therefore be expected. This is consistent with most findings in the literature and can be attributed to experimental errors and/or “precision manufacturing errors” (Brundrett, 1993) since handling screens is very delicate and any alteration in the location of weft or warp wires can have subsequent effects on the results. To be able to reduce such error, one should revert to meticulously measure all screen geometric parameters and conduct their experiments using “ideal” conditions.

Furthermore, this work also showed that several geometric parameters of the screens (e.g. porosity, hydraulic diameter, etc...) can be calculated using analytical equations (from general data provided by the manufacturer), and directly used in calculating the pressure drop without the need to experimentally measure them.

Declaration of Competing Interest

The authors declared that there is no conflict of interest.

Acknowledgment

The author would like to acknowledge the financial support of the Lebanese National Council for Scientific Research (CNRS-L) and the University Research Board at the American University of Beirut.

References

- Abou Hweij, K., Azizi, F., 2015. Hydrodynamics and residence time distribution of liquid flow in tubular reactors equipped with screen-type static mixers. *Chem. Eng. J.* 279, 948–963. <https://doi.org/10.1016/j.cej.2015.05.100>.
- Al Taweel, A.M., Chen, C., 1996. A novel static mixer for the effective dispersion of immiscible liquids. *Chem. Eng. Res. Des.* 74, 445–450.
- Al Taweel, A.M., Yan, J., Azizi, F., Odedra, D., Gomaa, H.G., 2005. Using in-line static mixers to intensify gas-liquid mass transfer processes. *Chem. Eng. Sci.* 60, 6378–6390. <https://doi.org/10.1016/j.ces.2005.03.011>.

- Al Taweel, A.M., Li, C., Gomaa, H.G., Yuet, P., 2007. Intensifying mass transfer between immiscible liquids: Using screen-type static mixers. *Chem. Eng. Res. Des.* 85, 760–765. <https://doi.org/10.1205/cherd06180>.
- Al Taweel, A.M., Azizi, F., Sirijeerachai, G., 2013. Static mixers: effective means for intensifying mass transfer limited reactions. *Chem. Eng. Process. Process Intensif.* 72, 51–62. <https://doi.org/10.1016/j.cep.2013.08.009>.
- Annand, W.J.D., 1953. The resistance to air flow of wire gauzes. *J. Aeronaut. Soc.* 57, 141–146.
- Armour, J.C., Cannon, J.N., 1968. Fluid flow through woven screens. *AIChE J.* 14, 415–420.
- Azizi, F., Al Taweel, A.M., 2007. Population balance simulation of gas-liquid contacting. *Chem. Eng. Sci.* 62, 7436–7445. <https://doi.org/10.1016/j.ces.2007.08.083>.
- Azizi, F., Al Taweel, A.M., 2011. Hydrodynamics of liquid flow through screens and screen-type static mixers. *Chem. Eng. Commun.* 198, 726–742. <https://doi.org/10.1080/00986445.2011.532748>.
- Azizi, F., Al Taweel, A.M., 2011. Turbulently flowing liquid-liquid dispersions. Part I: Drop breakage and coalescence. *Chem. Eng. J.* 166, 715–725. <https://doi.org/10.1016/j.cej.2010.11.050>.
- Azizi, F., Al Taweel, A.M., 2015. Mass transfer in an energy-efficient high-intensity gas-liquid contactor. *Ind. Eng. Chem. Res.* 54, 11635–11652. <https://doi.org/10.1021/acs.iecr.5b01078>.
- Bailey, B.J., Montero, J.J., Perez Parra, J., Robertson, A.P., Baeza, E., Kamaruddin, R., 2003. Airflow resistance of greenhouse ventilators with and without insect screens. *Biosyst. Eng.* 86, 217–229. [https://doi.org/10.1016/S1537-5110\(03\)00115-6](https://doi.org/10.1016/S1537-5110(03)00115-6).
- Bennani, A., Gence, J.N., Mathieu, J., 1985. Influence of a grid-generated turbulence on the development of chemical reactions. *AIChE J.* 31, 1157–1166.
- Bourne, J.R., Lips, M., 1991. Micromixing in grid-generated turbulence. Theoretical analysis and experimental study. *Chem. Eng. J. Biochem. Eng. J.* 47, 155–162.
- Brundrett, E., 1993. Prediction of pressure drop for incompressible flow through screens. *J. Fluids Eng.* 115, 239–242.
- Bussière, W., Rochette, D., Clain, S., André, P., Renard, J.B., 2017. Pressure drop measurements for woven metal mesh screens used in electrical safety switchgears. *Int. J. Heat Fluid Flow* 65, 60–72. <https://doi.org/10.1016/j.ijheatfluidflow.2017.02.008>.
- Carman, P.C., 1956. *Flow of Gases through Porous Media*. Academic Press.
- Castellano, S., Starace, G., De Pascalis, L., Lippolis, M., Scarascia Mugnozza, G., 2016. Test results and empirical correlations to account for air permeability of agricultural nets. *Biosyst. Eng.* 150, 131–141. <https://doi.org/10.1016/j.biosystemseng.2016.07.007>.
- Chen, C., 1996. Dispersion and coalescence in static mixers.
- Costa, S.C., Barrutia, H., Esnaola, J.A., Tutar, M., 2014. Numerical study of the heat transfer in wound woven wire matrix of a Stirling regenerator. *Energy Convers. Manag.* 79, 255–264. <https://doi.org/10.1016/j.enconman.2013.11.055>.
- de Vahl Davis, G., 1964. The flow of air through wire screens. *Hydraul. Fluid Mech.*, 191–212.
- Drevon, D., Fursa, S.R., Malcolm, A.L., 2017. Inter-coder reliability and validity of WebPlotDigitizer in extracting graphed data. *Behav. Modif.* 41, 323–339. <https://doi.org/10.1177/0145445516673998>.
- Eckert, B., Pfluger, F., 1942. Resistance Coefficients of Commercial Round Wire Grids (translated from Luftfahrtforschung), vol. 18, no. 4.
- Ehrhardt, G., 1983. Flow measurements for wire gauzes. *Int. Chem. Eng.* 23, 455–465.
- El-Ali, M.S., 2001. Performance Characteristics of a Novel Liquid-liquid Contactor. Dalhousie University.
- Ergun, S., 1952. Fluid flow through packed columns. *Chem. Eng. Prog.* 48, 89–94.
- Fischer, A., Gerstmann, J., 2013. Flow resistance of metallic screens in liquid. *Gaseous Cryogenic Flow*, 1–12.
- Grootenhuis, P., 1954. A correlation of the resistance to air flow of wire gauzes. *Proc. Inst. Mech. Eng.* 168 (1), 837–846. https://doi.org/10.1243/PIME_PROC_1954_168_076_02.
- Groth, J., Johansson, A.V., 1988. Turbulence reduction by screens. *J. Fluid Mech.* 197, 139–155. <https://doi.org/10.1017/S0022112088003209>.
- Ingmanson, W.L., Han, S.T., Wilder, H.D., Myers Jr., W.T., 1961. Resistance of wire screens to flow of water. *Tappi*. 44, 47–54.
- Kołodziej, A., Łojewska, J., 2009. Experimental and modelling study on flow resistance of wire gauzes. *Chem. Eng. Process. Process Intensif.* 48, 816–822. <https://doi.org/10.1016/j.cep.2008.10.009>.
- Kołodziej, A., Jaroszyński, M., Janus, B., Kleszcz, T., Łojewska, J., Łojewski, T., 2009. An experimental study of the pressure drop in fluid flows through wire gauzes. *Chem. Eng. Commun.* 196, 932–949. <https://doi.org/10.1080/00986440902743851>.
- Kołodziej, A., Łojewska, J., 2009. Flow resistance of wire gauzes. *AIChE J.* 55, 264–267. <https://doi.org/10.1002/aic>.
- Kołodziej, A., Łojewska, J., Jaroszyński, M., Gancarczyk, A., Jodłowski, P., 2012. Heat transfer and flow resistance for stacked wire gauzes: experiments and modelling. *Int. J. Heat Fluid Flow* 33, 101–108. <https://doi.org/10.1016/j.ijheatfluidflow.2011.11.006>.
- Kurian, T., Fransson, J.H.M., 2009. Grid-generated turbulence revisited. *Fluid Dyn. Res.* 41, 021403. <https://doi.org/10.1088/0169-5983/41/2/021403>.
- Laws, E.M., Livesey, J.L., 1978. Flow through screens. *Annu. Rev. Fluid Mech.* 10, 247–266. <https://doi.org/10.1146/annurev.fl.10.010178.001335>.
- Li, H.Z., Fasol, C., Choplin, L., 1997. Pressure drop of newtonian and non-newtonian fluids across a sulzer SMX static mixer. *Chem. Eng. Res. Des.* 75, 792–796. <https://doi.org/10.1205/026387697524461>.
- Munson, B.R., 1988. Very low Reynolds number flow through screens. *J. Fluids Eng.* 110, 462–463.
- Okolo, P.N., Zhao, K., Kennedy, J., Bennett, G.J., 2019. Numerical assessment of flow control capabilities of three dimensional woven wire mesh screens. *Eur. J. Mech. B/Fluids* 76, 259–271. <https://doi.org/10.1016/j.euromechflu.2019.03.001>.
- Pinker, R.A., Herbert, M.V., 1967. Pressure loss associated with compressible flow through square-mesh wire gauzes. *J. Mech. Eng. Sci.* 9, 11–23.
- Roach, P.E., 1987. The generation of nearly isotropic turbulence by means of grids. *Int. J. Heat Fluid Flow* 8, 82–92. [https://doi.org/10.1016/0142-727X\(87\)90001-4](https://doi.org/10.1016/0142-727X(87)90001-4).
- Schubauer, G.B., Spangenberg, W.G., Klebanoff, P.S., 1950. Aerodynamic Characteristics of Damping Screens. <https://ntrs.nasa.gov/search.jsp?R=19930082665>.
- Simmons, L.F.G., Cowdrey, C.F., 1945. Measurements of the Aerodynamic Forces Acting on Porous Screens. R. & M. No. 2276, Br. ARC, Aug. (1945).
- Taylor, G.I., Davies, R.M., 1944. The aerodynamics of porous sheets, Aeronaut. Res. Council. Reports Memo.
- Teitel, M., 2010. Using computational fluid dynamics simulations to determine pressure drops on woven screens. *Biosyst. Eng.* 105, 172–179. <https://doi.org/10.1016/j.biosystemseng.2009.10.005>.
- Teitel, M., Dvorkin, D., Haim, Y., Tanny, J., Seginer, I., 2009. Comparison of measured and simulated flow through screens: effects of screen inclination and porosity. *Biosyst. Eng.* 104, 404–416. <https://doi.org/10.1016/j.biosystemseng.2009.07.006>.
- Thakur, R.K., Vial, C., Nigam, K.D.P., Nauman, E.B., Djelveh, G., 2003. Static mixers in the process industries—a review. *Trans. IChemE* 81, 787–826.
- Theron, F., Le Sauze, N., 2011. Comparison between three static mixers for emulsification in turbulent flow. *Int. J. Multiph. Flow* 37, 488–500. <https://doi.org/10.1016/j.ijmultiphaseflow.2011.01.004>.
- Valera, D.L., Molina, F.D., Álvarez, A.J., López, J.A., Terrés-Nicoli, J.M., Madueño, A., 2005. Contribution to characterisation of insect-proof screens: experimental measurements in wind tunnel and CFD simulation. *Acta Hort.* 691, 441–448. <https://doi.org/10.17660/ActaHortic.2005.691.53>.
- Wakeland, R.S., Keolian, R.M., 2003. Measurements of resistance of individual square-mesh screens to oscillating flow at low and intermediate reynolds numbers. *J. Fluids Eng.* 125, 851–862. <https://doi.org/10.1115/1.1601254>.
- Wiegardt, K.E.G., 1953. On the resistance of screens. *Aeronaut. Q.* 4, 186–192.
- Wu, W.T., Liu, J.F., Li, W.J., Hsieh, W.H., 2005. Measurement and correlation of hydraulic resistance of flow through woven metal screens. *Int. J. Heat Mass Transf.* 48, 3008–3017. <https://doi.org/10.1016/j.ijheatmasstransfer.2005.01.038>.